CHAPTER - 3

TERCOPOLYMERIZATION OF ACRYLAMIDE, ACRYLIC ACID AND ACRYLONITRILE : SYNTHESIS AND PROPERTIES

3.1 Preview

3.2 Materials

3.3 Experimental Techniques

3.4 Synthesis of Polymers

3.5 Results and Discussion

(a) IR analysis
(b) ^{1}H-NMR analysis
(c) ^{13}C-NMR analysis
(d) TGA analysis
(e) DSC analysis
(f) Viscosity measurements
(g) Biodegradation measurements

3.6 Conclusion

3.7 References

3.1 Preview

Research on polymers has been mainly addressed to the synthesis of new materials with specific performance for last 30 years. A wide variety of chemical or physical strategies including copolymerization, polymer blends and composites, or crosslinking networks have been explored to match the individual requirements[1]. Tercopolymerizations have continued to evoke interest by both academics and industrialists. One of the main advantages of this technique is that it provides a convenient method of synthesizing new polymeric structures with wide ranges of properties[2]. Although extensive literature is available for homo- and copolymerization, very little kinetic or synthetic information is available for tercopolymerization[3]. As it becomes more and more possible to "*tailor-made*" polymers with specific physical and chemical properties, it will undoubtedly become necessary to resort to such multiple combinations wherein each monomer contributes some particular property or properties. Interest in multifunctional synthetic polymers or copolymers is steadily increasing, as macromolecular catalysts, macromolecular drugs or antimetastatic agents[4]. Such activated drug-binding matrices are usually based on N-acryloyloxypthalamides and N-metha cryloyloxyphthalimide with methyl acrylate and acrylonitrile as comonomers. The tercopolymerization of maleic anhydride-methyl methacrylate-styrene has been studied extensively and modified by tributyltin oxide to yield tercopolymers of biological interest[5]. The growth in the production of plastic materials during the past few years has been accompanied by an increased demand for materials with improved physical and mechanical properties,

---

Parts of this Chapter were published in J. Appl Polym. Sci., 69, 217 (1998); in THERMANS 98, p.212 and in Polymer International (accepted for publication)

greater heat and radiation stability, etc. Only a few homopolymers answer such demands. In this respect, the tercopolymerization of acrylonitrile, styrene, and esters of α-cyanocinnamic acid has been reported[6]. Prasad et al.[7] studied the microstructure of poly(acrylonitrile-methyl methacrylate-itaconic acid) using ^{13}C-NMR technique. Recently, the water uptake and swelling behavior of physically crosslinked, inhomogeneous poly(acrylonitrile-acrylamide-acrylic acid) hydrogels have been reported[8].

To create materials that continue to have strength and functionality while in service but degrade after use is a rather novel concept in the development of materials[9,10]. Among water soluble synthetic polymers, the biodegradability of polyvinyl alcohol[11,12] and polyethylene glycol[13 14] has been studied in detail by using microorganisms. Polyacrylates and polymethacrylates generally resist biodegradation[15]. Weight loss in soil burial tests has been reported for copolymers of ethylene and propylene with acrylic acid, acrylonitrile and acrylamide[16]. Studies on biodegradation of copolymers of acrylonitrile-dimethyl aminoethyl methacrylate, acrylonitrile-acrylic acid[17], polyacrylates[18,19], poly methyl cyanoacrylate[20] and the oligomers of sodium acrylate[21] are available. Interestingly, in a recent report[22], hydroxyquinoneperoxidase of a lignin degrading bacterium Azotobacter beijrinkii HM 121 has been shown to degrade polyacrylamide and polyacrylic acid.

In this chapter, we report on the synthesis and properties of tercopolymers of acrylamide, acrylonitrile, and acrylic acid from various feed ratios. These polymers have been characterized by elemental analysis, IR, ^{1}H- and ^{13}C-NMR spectroscopy, TGA and DSC analysis, viscosity measurements and

observations in support of the biodegradable nature of these polymers. This is because a) it is suggested[23,24] that ^{13}C-NMR is one of the most useful and reliable techniques for the characterization of the polymer structure. The large chemical shift range in ^{13}C-NMR permits the study of more complex systems and the elucidation of detailed structural information, b) The thermogravimetric analysis (TGA) is widely used to investigate the thermal decomposition of polymers and associated kinetic parameters and c) Viscosity of dilute polymer solution gives an insight of the conformation adopted by polymer chain. The changes in the physical and chemical properties as a function of the chemical composition are studied and presented in detail.

3.2 Materials

Acrylamide (Mitsubishi Chemicals Ltd.), acrylic acid (National Chemicals, Baroda, India), and acrylonitrile (BDH, Poole, England) were used for the polymerization without any prior purification. Benzoyl peroxide (National Chemicals, Baroda, India) was purified by dissolving it in chloroform at room temperature and reprecipitating it by adding methanol, before it is used in the polymerization process. Hydrogen peroxide (Glaxo, Mumbai, India, 100 vol. i.e. 30% w/v) was used as received. The solvents were freshly distilled prior to use.

3.3 Experimental Techniques

IR spectra of the films of the homopolymers and tercopolymers were recorded on a Perkin-Elmer 16PC spectrophotometer. The films were prepared by dissolving the polymer in a mixture of DMF : H_2O (60 : 40, v/v) and pouring the solution over a pool of mercury. The films were obtained by vacuum evaporation of the solvent.

The NMR of the polymer solutions was recorded on a JEOL GSX, 400 MHz for PMR at the RSIC, IIT, Madras, India. ^{13}C-NMR spectra was recorded for samples of homopolymers of AA, AN and their tercopolymers with AM having 20-25% (w/v) solution in D_2O and DMSO-d_6 at 90°C on a JEOL JNM FX-100 FT-NMR spectrometer at a frequency of 25 MHz. TMS was used as an internal reference, while D_2O and DMSO-d_6 acted as internal lock. Elemental analysis was done on a Hearaous, RAPID (made in Germany) C, H, N, O, analyzer at S.P.University, Vallabh Vidyanagar, India.

TGA was recorded with a Shimadzu thermal analyzer DT-30B. The TGA analysis was done under a nitrogen atmosphere. DSC was recorded on a Mettler-TC 22 in the presence of nitrogen gas at 10 K min^{-1}. Viscosity studies of different solutions were carried out with the help of an Ubbelohde viscometer, placed vertically in a thermostat, at all required temperatures (± 0.05°C).

In the biodegradation studies, minimal salt medium (1L, pH 7.0) which contained [g/L] 4.3 K_2HPO_4, 3.4 KH_2PO_4, 0.3 $MgCl_2.H_2O$, and 0.5 mL of trace element solution having [mg/L] 1.0 $MnCl_2.4H_2O$, 0.6 $FeSO_4.7H_2O$, 2.6 $CaCl_2.H_2O$, 6.0 $NaMoO_4$ was used[25] for growth and respiration studies. Ammonium sulphate [1.0 g/L] was supplied as a nitrogen source. Different tercopolymers were added to the above medium as the sole source of carbon and energy and the medium was sterilised by autoclaving at 10 psi for 20 min. Minimal medium without the polymer was also inoculated and served as a control.

Following the conventional baiting technique[26] and using the water insoluble polymer IV (i.e. TP4) suspended in minimal medium without carbon source as a bait, a soil bacterium designated here as BA-1 capable of growing on tercopolymers was enriched and isolated. The procedure followed for this is : approximately 100 mg of polymer IV (i.e. TP4) granule was suspended into a soil suspension in the minimal medium and inoculated for 72h at static condition at 28 ± 2^0C.The granule was given further two transfers in the minimal medium at an interval of 72h. The supernatant was then streaked onto Luria Agar plates and the organism was isolated and designated as BA-1.

For growth studies, cultures were cultivated in 5.0 mL of the minimal medium in 50 mL culture tubes at 30°C on a rotary shaker at 180 rpm. The growth was followed turbidimetrically at 600 nm.

Tercopolymer dependent respiratory activity was followed polarographically using a Gilson Oxygraph. Reaction chamber fitted with Clark type oxygen electrode contained: minimal medium, washed cell suspension and the respective polymers at a final concentration of 0.5% (w/v) in a total volume of 1.4 mL at 30°C. Cells used in this study were grown in the respective polymers.

For whole-cell protein determination, cellular proteins were solubilised by treating the cells with alkali (approx. 100 μg dry weight/ 0.5 mL + 0.5 mL of 1.0 N NaOH) at 100°C for 5 min and were subsequently estimated by the method of Lowry et al[27].

For the detection of degradation products, the bacteria were grown on the respective polymers for 3 days. After removing the bacterial cells by centrifugation of the culture broth at 10,000 rpm for 30 min, the unused

polymer was precipitated with 10 volumes of methanol, the precipitate was removed by centrifugation at 10,000 rpm for 20 min. The supernatant was then concentrated at 70°C to 1.0 mL and analysed subsequently by gas chromatography for the presence of acrylamide, acrylic acid and acrylonitrile.

Gas chromatography was performed on a Perkin-Elmer Autosystem equipped with a flame ionisation detector. Acrylamide and acrylic acid were analysed by the following temperature program, using the BP5 capillary column (25 mts, 0.53 mm i.d): Temperature was held at 60°C for 1 min after injection of the sample (1μL) and increased to 130°C at the rate of 6°C min^{-1} and then maintained at this temperature for 1 min. Acrylonitrile was analysed using a Carbowax 20M column by the following temperature program: After injection of the sample (1μL) the initial column temperature was held at 50°C for 1 min., increased then to 60° C at the rate of 2°C min^{-1} and finally to 150°C at the rate of 20°C min^{-1}. Injector temperature for all the samples was maintained at 200°C.

3.4 Polymer Synthesis

The synthesis of the homopolymers polyacrylic acid (PAA)[28] and polyacrylamide (PAM)[29,30] was done as reported in the literature. The synthesis of polyacrylonitrile (PAN) was carried out as reported earlier[31,32]. Polyacrylamide (PAM) was synthesized by taking 20% (w/v) of acrylamide in water in presence of 10 mL H_2O_2 (3%, w/v). the whole set up constituted of a three necked flask, equipped with a stirrer, water condenser, and a nitrogen inlet. The flask was maintained at a desired temperature in a thermostated water bath. The reaction mixture was stirred at 82^0C for a period of one half hour. The reaction mixture after polymerization was poured into excess of methanol.

Synthesis of polyacrylic acid (PAA) was carried out using potassium persulfate as the initiator, 40 g of acrylic acid in 160 mL water was taken in a three necked flask. The reaction set up was maintained as before. The reaction mass was poured into excess of acetone to precipitate out the product. It was washed with excess of acetone. The product obtained was again dissolved in solvent water and the product was dried by freeze drying technique. This method was used for drying in order to avoid cross linking of the polymer. In this manner, the product obtained was water soluble polyacrylic acid.

The synthesis of polyacrylonitrile (PAN) was carried out in the following way : Ten grams of AN and 0.1 g of benzoyl peroxide (BPO) in 50 mL of DMF was taken in a three necked flask. The reaction set up was maintained as before. The reaction mixture was stirred for a period of 5 h, under a nitrogen atmosphere, at 85^0C. PAN was obtained by pouring the reaction mixture into nonsolvent methanol.

The synthesis of tercopolymers was carried out in various monomer feed ratios of (TP1) 80:10:10, (TP2) 60:20:20, (TP3) 40:30:30, and (TP4) 20:40:40 (w/w/w) of acrylamide (AM), acrylic acid (AA), and acrylonitrile (AN), respectively. The solution polymerization was carried out in a mixture of DMF and water (60:40, v/v) under the nitrogen atmosphere. The monomer-to-solvent ratio was 1:4 (w/v). The initiator benzoyl peroxide concentration was 1.0% (w/w) to total monomer weight. The reactor set up consisted of a three necked round-bottom flask equipped with a water condenser at one side neck and the N_2 inlet at the other. The reaction mixture was mechanically stirred through the center neck. The whole assembly was placed in a thermostated water bath at 85°C. The reaction time was 8 h. After polymerization, the reaction mass, for

samples TP1 and TP2, was poured into an excess of methanol, and for samples TP3 and TP4, it was poured into an excess of distilled water. The reprecipitated products were Soxhlet-extracted with various solvents to remove the respective homo- and copolymers. The purification procedure of samples TP1 and TP2 is schematically shown in Figure 3.1, and that of samples TP3 and TP4 is shown in Figure 3.2. All the homo- and tercopolymers were dried in vacuo and then characterized.

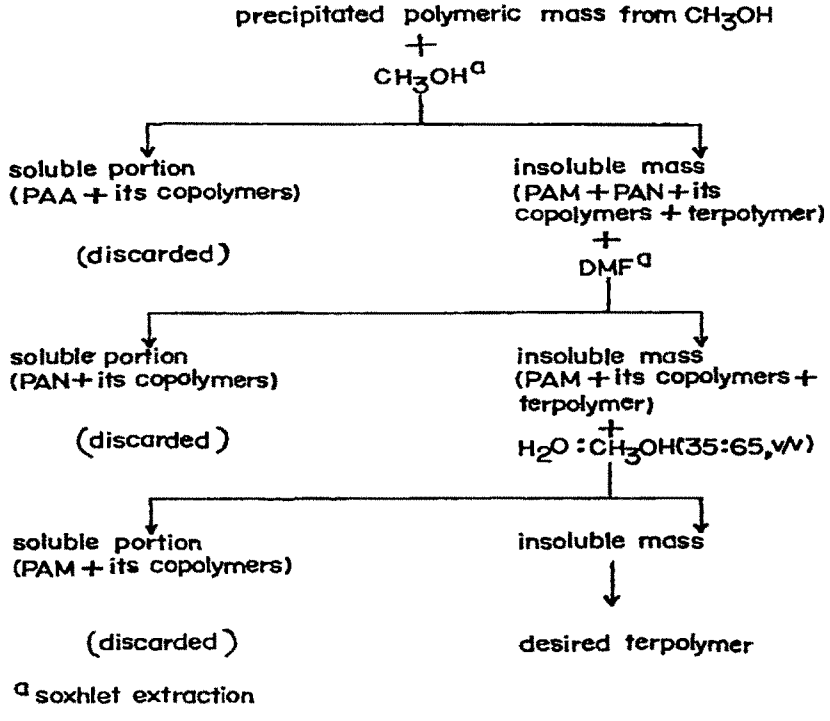

Figure 3.1 : Schematic representation of purification of tercopolymers TP1 and TP2.

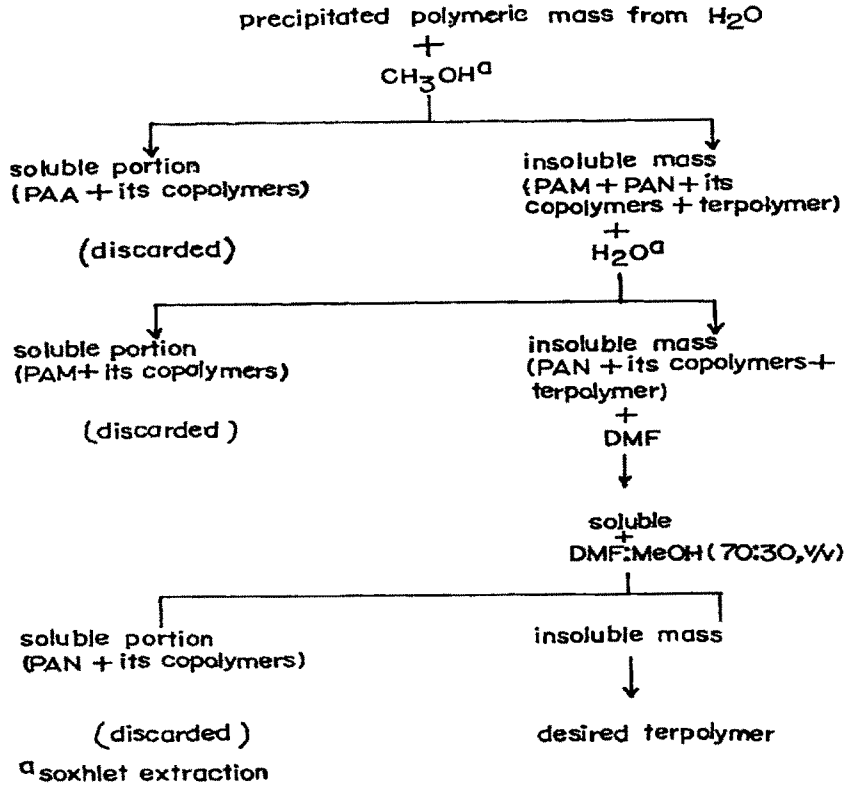

Figure 3.2 : Schematic representation of purification of tercopolymers TP3 and TP4.

3.5 Results and Discussion

(a) IR analysis :

The homopolymers PAM, PAN, and PAA showed characteristic IR absorptions, which agreed very well with those reported in the literature (Figures 3.3 and 3.4). PAN showed strong absorptions at 2246 and 1452 cm^{-1} due to the nitrile group. The C=O band of PAA was observed at 1738 cm^{-1}. Besides this, the broad absorption band due to the O-H of the -COOH group was observed around 3300 cm^{-1}. The IR spectrum of PAM showed strong absorption at 1650 cm^{-1} due to the C=O bond of the carbonamide group. The

medium absorption at 1400 cm^{-1} was due to the C-N stretch. Representative IR spectra of tercopolymers TP2 (AM : AA : AN = 60 : 20 : 20) and TP3 (AM : AA : AN = 40 : 30 : 30) are given in Figures 3.3 and 3.4. The characteristic absorption peaks due to the three functional groups were present in all the tercopolymers studied.

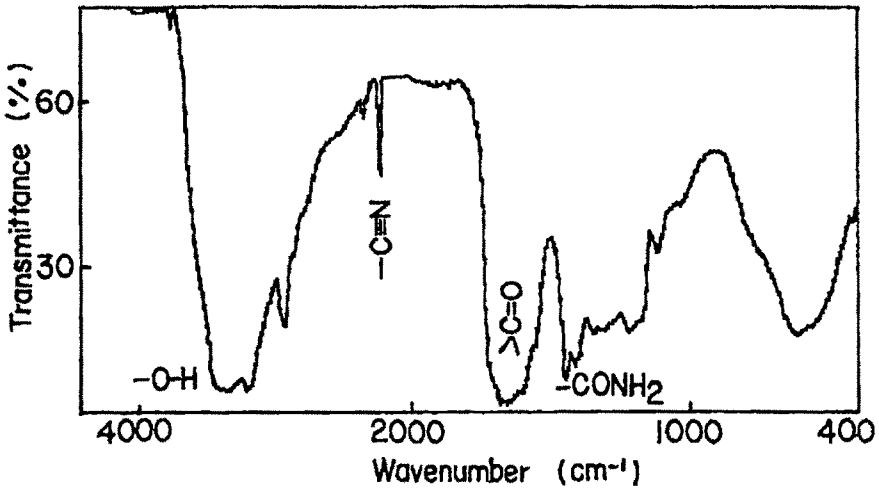

Figure 3.3 : Representative IR spectrum of tercopolymer TP2

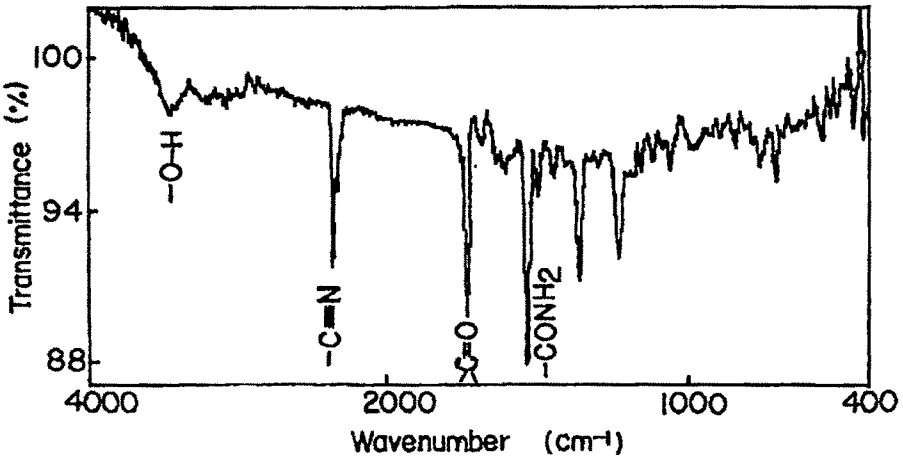

Figure 3.4 : Representative IR spectrum of tercopolymer TP3.

(b) ^{1}H-NMR analysis:

Further evidence for the three monomers incorporated was given by the ^{1}H-NMR spectra of the tercopolymers (Figures 3.5 and 3.6). In the ^{1}H-NMR spectra of PAM, the methylene protons appeared as a broad peak at δ = 1.6 - 1.8 ppm[33]. The methine protons resonate at δ = 2.28 ppm. The ^{1}H-NMR spectrum of PAN shows peaks at δ = 2.07 ppm due to methylene protons and due to methine protons at δ = 3.12 ppm. In the presence of monomer AA, the methylene signal shifted downfield to δ = 2.06; the methine proton remain at δ = 3.12 ppm[34]. In the case of tercopolymers (Figs. 3.5 and 3.6), a broad peak appeared in the range of δ = 1.4 - 2.0 due to methylene groups of AM. A sharp peak was observed due to the methine of the AA comonomer at δ = 2.75 ppm and at δ = 2.93 due to the AN comonomer. As the ratio of AA and AN increases, the intensity of the peak height increases in the expected direction.

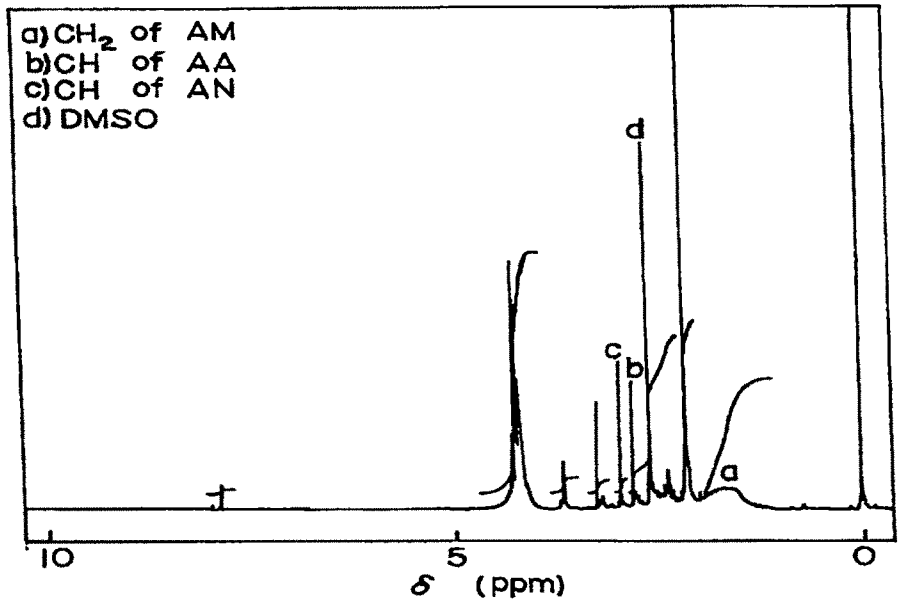

Figure 3.5 : ^{1}H-NMR spectrum of tercopolymer TP2.

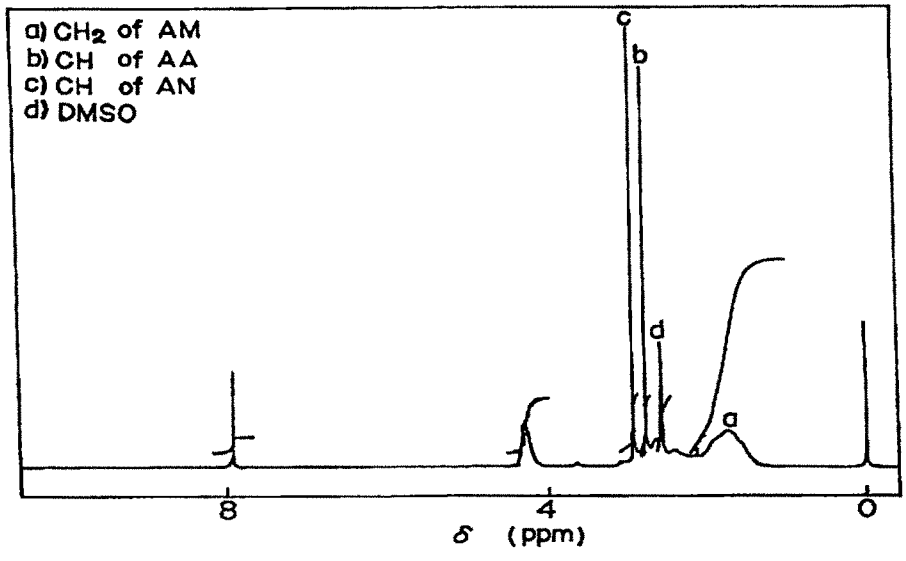

Figure 3.6 : ^{1}H-NMR spectrum of tercopolymer TP3.

The experimental feed ratios of various monomers as well as the composition of the resulting tercopolymers, obtained by elemental analysis, are summarized in Table 3.1. The reactivity ratios (r) of (AA + AN) and AM in the tercopolymer were estimated by the graphical method of Kelen-Tudos[35] :

$$\theta = r_1\varepsilon - r_2 (1 - \varepsilon) / \gamma \qquad (1)$$

where 1 stands for (AA + AN) and 2 for AM. θ, ε, and γ are mathematical functions of G and F as defined in Table 3.2. On plotting θ versus ε, a linear plot was obtained. The intercepts at $\varepsilon = 0$ and $\varepsilon = 1$ gave $-r_2/\gamma$ and r_1, respectively. The values obtained for r_1 and r_2 were $r_1 = 0.86 \pm 0.09$ and $r_2 = 1.93 \pm 0.03$.

The reactivity ratios r_1 and r_2 were also determined by the Fineman-Ross[36,37] method. The following equation was used :

Table 3.1 : Composition of AM, AA and AN in Feed and in Tercopolymers.

	Polymer Samples	Mol Fraction (M) of AM, AA and AN in Feed			Elemental Analysis		Mol Fraction of (Ø) of AM, AA and AN in Tercopolymer (Experimental)		
		(M_{AM})	(M_{AA})	(M_{AN})	N (%)	O (%)	($Ø_{AM}$)	($Ø_{AA}$)	($Ø_{AN}$)
TP1	AM-AA-AN (80 : 10 : 10)	0.775	0.096	0.130	17.14	25.31	0.861	0.130	0.009
TP2	AM-AA-AN (60 : 20 : 20)	0.563	0.185	0.251	17.27	22.18	0.568	0.179	0.254
TP3	AM-AA-AN (40 : 30 : 30)	0.364	0.270	0.366	14.91	24.76	0.446	0.291	0.262
TP4	AM-AA-AN (20 : 40 : 40)	0.177	0.349	0.474	14.08	23.61	0.224	0.358	0.417
	PAM	--	--	--	18.12	25.61	--	--	--
	PAN	--	--	--	25.39	--	--	--	--

Table 3.2 : Kelen-Tudos Parameters for AM and for AA + AN

Samples	$X = \frac{M_1}{M_2}$	$Y = \frac{\phi_1}{\phi_2}$	$G = \frac{X(Y-1)}{Y}$	$F = \frac{X^2}{Y}$	$\varepsilon = \frac{F}{\gamma^a + F}$	$\theta = \frac{G}{\gamma^a + F}$
TP1	0.29	0.16	-1.51	0.53	0.23	-0.65
TP2	0.77	0.76	--	--	--	--
TP3	1.75	1.24	0.34	2.46	0.58	0.08
TP4	4.65	3.46	3.31	6.25	0.77	0.41

$^a\gamma = \sqrt{F_{max}\, F_{min}} = 1.81$: M_1 is the mole fraction of AA + AN and M_2 is the mole fractions of AM in feed; ϕ_1 and ϕ_2 are their respective experimental mole fractions in the tercopolymer.
See Table 3.1 and text for symbols.

$$X(Y - 1) / Y = r_1 (X^2 / Y) - r_2 \quad (2)$$

where $X = M_1/M_2$ and $Y = \varnothing_1 / \varnothing_2$ (as defined in Table 3.2).

On plotting $X(Y - 1)/Y$ against X^2/Y, a straight line was obtained, whose slope was r_1 and the intercept yielded r_2. The values obtained for r_1 and r_2 are 0.86 ± 0.05 and 1.94 ± 0.09, respectively. The r_1r_2 value indicates that the tercopolymers are block copolymers of AM and (AA + AN) which are rich in AM[37].

The statistical distributions of the monomer sequences 1-1, 2-2, and 1-2 were calculated using the following relations[38-40] :

$$X' = \varnothing_1 - 2\varnothing_1\varnothing_2 / \{1 + [(2\varnothing_1 - 1)^2 + 4r_1r_2\varnothing_1\varnothing_2]^{1/2}\} \quad (3)$$

$$Y' = \varnothing_2 - 2\varnothing_1\varnothing_2 / \{1 + [(2\varnothing_1 - 1)^2 + 4r_1r_2\varnothing_1\varnothing_2]^{1/2}\} \quad (4)$$

$$Z' = 4\varnothing_1\varnothing_2 / \{1 + [(2\varnothing_1 - 1)^2 + 4r_1r_2\varnothing_1\varnothing_2]^{1/2}\} \quad (5)$$

where $\varnothing_1$ is the mol fraction of AA and AN together and $\varnothing_2$ is the mol fraction of AM when the blockiness between these are considered in the tercopolymers. The mol fractions of 1-1, 2-2, and 1-2 are designated by X′, Y′, and Z′, as listed in Table 3.3. The mean sequence lengths μ_1 and μ_2 were calculated utilizing the relations

$$\mu_1 = 1 + r_1 (\varnothing_1)/(\varnothing_2) \quad (6)$$

$$\mu_2 = 1 + r_2 (\varnothing_2)/(\varnothing_1) \quad (7)$$

The calculated values are listed in Table 3.3.

(c) ^{13}C-NMR analysis :

The incorporation of all the three monomers i.e. acrylamide (AM), acrylic acid (AA) and acrylonitrile (AN) in the tercopolymers is evident from ^{13}C-NMR spectral data. The ^{13}C-NMR spectra of homopolymers of AN and AA and their

Table 3.3 : Structural Data for the Terpolymers of AM and of AA + AN

Polymer Samples	Composition[a] (Mole Fraction)		Blockiness[b] (Mole Fraction)		Alternation[b] (Mole Fraction)	Mean Sequence length		$\frac{\mu_1}{\mu_2}$
	ϕ_1	ϕ_2	1-1 (X')	2-2 (Y')	1-2 (Z')	μ_1	μ_2	
TP1	0.14	0.86	0.028	0.748	0.224	1.1	12.9	0.1
TP2	0.43	0.57	0.215	0.355	0.429	1.6	3.6	0.5
TP3	0.55	0.45	0.333	0.233	0.433	2.1	2.6	0.8
TP4	0.78	0.22	0.624	0.064	0.311	4.1	1.5	2.6

[a] From elemental analysis.
[b] Statistically calculated using reactivity ratios.
See Table 3.1 and text for symbols.

tercopolymers with AM are shown in Fig. 3.7. In the Polyacrylonitrile (PAN) homopolymer [Fig. 3.7(d)], methylene (βCH_2-) carbon appeared at δ = 32.86 ppm. The methine (αCH-) carbon giving rise to three well resolved peaks centred at δ = 27.44 ppm due to triad chemical shift sensitivity[41]. The nitrile (-CN) carbon in PAN appeared as a multiplet in the region δ = 119.53-120.17 ppm. Different peaks in the nitrile carbon signal are due to iso-, hetero- and syndiotactic triads with iso- appearing at a higher shift. However, in methine signals the iso- appears at a lower magnetic field followed by hetero and syndiotactic signals at higher magnetic fields, respectively[34]. The Polyacrylic acid (PAA) homopolymer [Fig.3.7(a)] shows three well resolved peaks at δ = 176.11, 39.13 and 31.91 ppm corresponding to carbonyl, methine and methylene carbons respectively.

In case of tercopolymer [TP1, Fig. 3.7(b)] an extra peak due to methine (αCH-) carbon of the backbone of AM resonates at 44.72 ppm and the backbone methylene (βCH_2-) carbon resonates at 40.59 ppm and overlaps with methine (αCH-) carbon of AA moiety present in the tercopolymers. Whereas, absorption of methylene carbon of AA overlapped with methine carbon of AN and hence could not be distinguished in ^{13}C-NMR spectra.. The two distinct signals due to carbonyl carbons of -$CONH_2$ and -COOH groups appear at δ = 175.94 and 174.30 ppm respectively. All other carbons in the tercopolymer chain in the 36-42 ppm range were overlapped by DMSO and hence could not be resolved[42] [Fig. 3.7(c)]. As the concentration ratio AA/AM in the tercopolymers increases, the ratio of corresponding peak heights also increases.

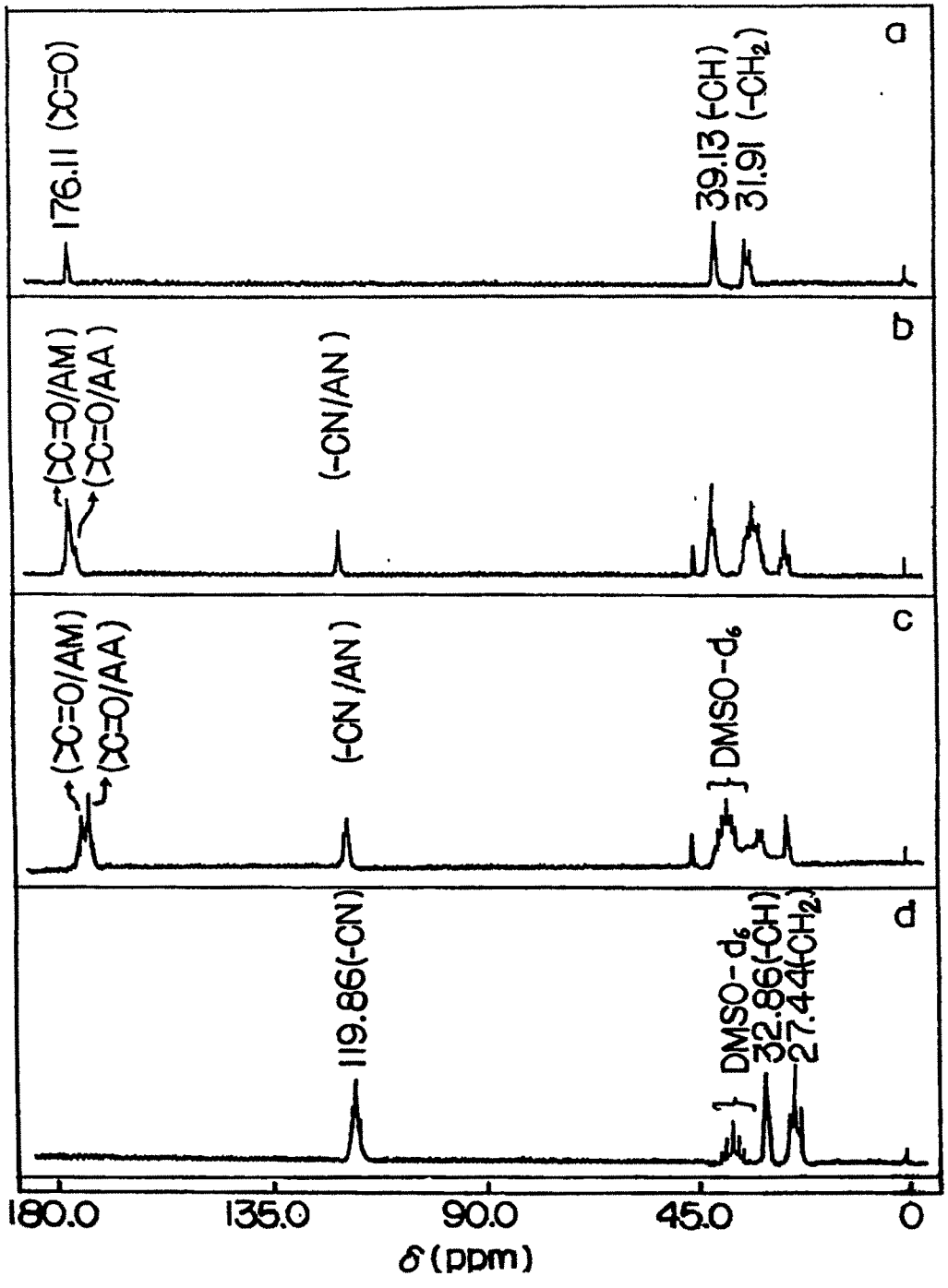

Figure 3.7 : ^{13}C-NMR spectra of homopolymers andtercopolymers (a) PAA, (b) tercopolymer TP1 in D_2O and (c) tercopolymer TP4 and (d) PAN in DMSO-d_6.

(d) TGA analysis :

The TGA of PAM, PAA, PAN, and tercopolymer IV (TP4) are given in Figure 3.8(a) and all the tercopolymers together are given in Figure 3.8(b). As observed in Figure 3.8(a), the thermogram of tercopolymer IV (TP4) falls in between those of its homopolymers, indicating a somewhat intermediate thermal stability. Other tercopolymers also show intermediate thermal stability. Two-stage decomposition was observed in all cases, except PAM. The first-stage decomposition of PAA started around 260°C. This is due to the formation of anhydride linkages. Similar values were reported earlier for PAA[43]. Heating above 350°C results in rapid decomposition to monomer, carbon dioxide, and volatile hydrocarbons. The TGA of PAM was three-staged, as observed before[44]. First, the loss of water, which is nonstoichiometric occurred. This is followed by the subsequent loss of ammonia and other gaseous products from the PAN structure formed during the decomposition of PAM and partly from the remaining PAM in the course of heating to 600°C[45].

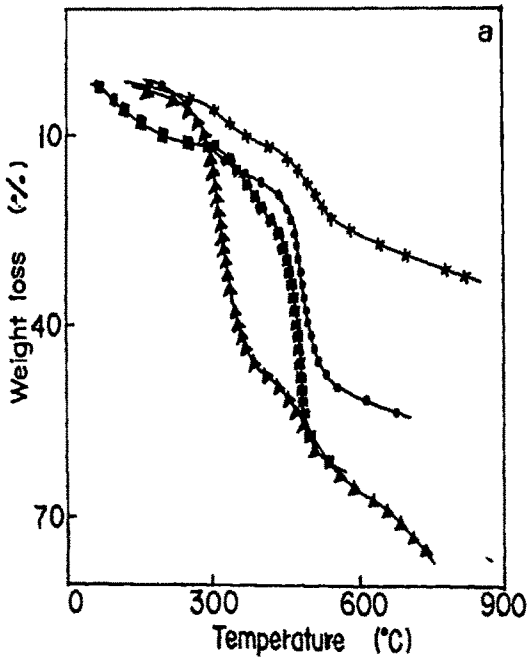

Figure 3.8(a): Representative TGA plots of (■) PAM, (▲) PAA,(X) PAN, and (●) tercopolymer IV (TP4) at heating rate of 10 K min^{-1} in N_2 atmosphere.

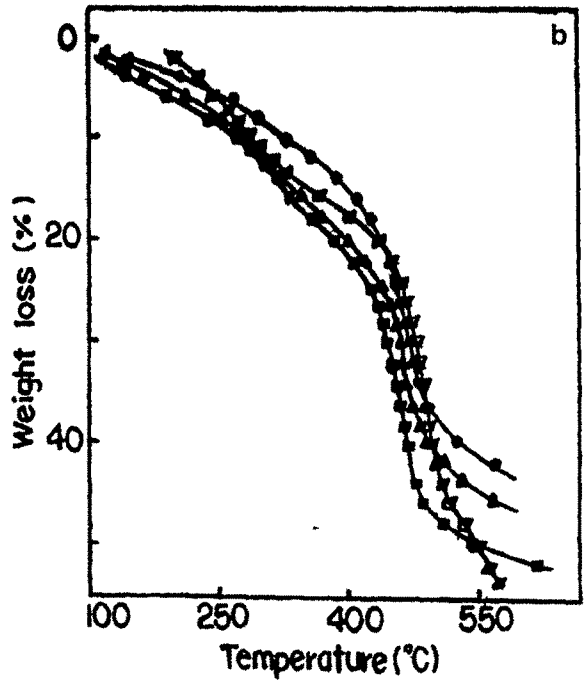

Figure 3.8(b) : Representative TGA plots of tercopolymers (■) TP1, (▲) TP2, (●) TP3 and (⊡) TP4 at heating rate of 10 K min^{-1} in N_2 atmosphere.

The various methods available[46-53] to estimate kinetic parameters to thermal decomposition use the following form of equation

$$-dW/dt = A \exp(E_a/RT)\, W^x \qquad (8)$$

where, W is the fractional residual weight of the sample, T is the absolute temperature, R is the gas constant, t is the time and A, E_a and x are the pre-exponential factor, the activation energy and the order of reaction respectively. It is, however, not clear yet as to which of the methods is the most suitable (proper) method for describing the thermal decomposition of the polymers.

The Ozawa[46-48] method, a dynamic analysis technique, was used for the determination of the activation energy. Thermograms were recorded at various

heating rates of 10, 15, and 20 K min^{-1} in N_2. The fraction of decomposition α, was obtained by the following equation:

$$\alpha = (W_o - W_t) / (W_o - W_f) \qquad (9)$$

where W_o is the initial weight of the polymer, W_t is the weight of polymer at temperature t; and W_f, the final weight. The $(1 - \alpha)$ values were found for each heating rate from the TG curves; the $(1 - \alpha)$ values, hence, obtained were plotted against 1/T.The equation used in this case is

$$-\log\beta = 0.4567\, E_a/RT + \text{Constant} \qquad (10)$$

where β is the heating rate. According to the Ozawa method[46-48], the plot of log β against the reciprocal of absolute temperature, for different values of $(1 - \alpha)$, is linear. The activation energy (E_a) of the decomposition was obtained from the slope of above linear plot. The plot of log β versus 1/T, for tercopolymer IV (TP4) at different values of $(1 - \alpha)$, each differing by 0.05, is shown in Figure 3.9(a). The activation energy at different $(1 - \alpha)$ are given in Table 3.4. For tercopolymers, the activation energy was independent of the fraction of decomposition. In tercopolymer IV (TP4), where the AA and AN feed ratios are higher, the E_a values are much higher than the rest, indicating a synergistic effect of its stability. A high stability of PAN in a nitrogen atmosphere was observed. The PAA and PAM have almost the same stability though lower than PAN in the presence of nitrogen.

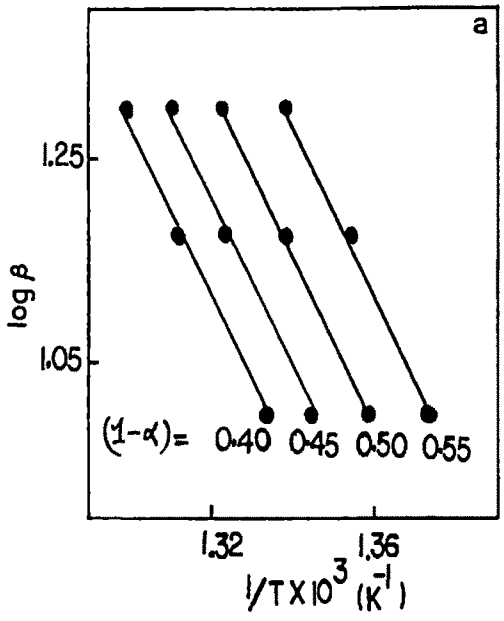

Figure 3.9(a) : Representative Ozawa plot of log β against 1/T for tercopolymer TP4 at different (1-α) values (see text)

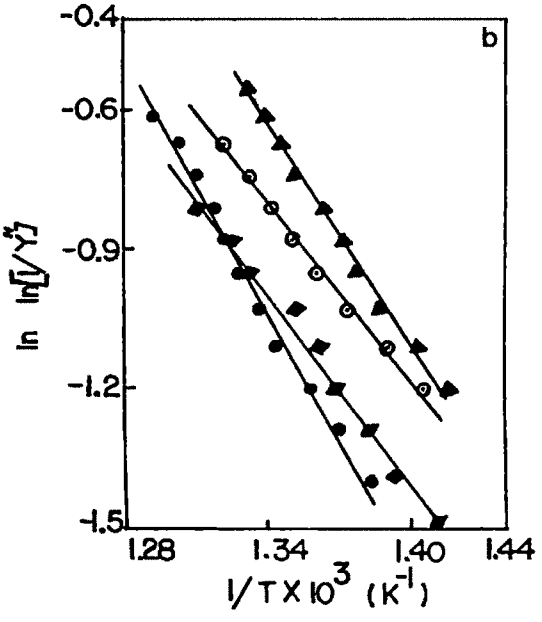

Figure 3.9(b) : Broido plot for tercopolymers : (▲) TP1; (□) TP2; (■) TP3; (●) TP4 (see text)

The activation energy associated with each stage of decomposition was also evaluated by the well-known Broido method[49]. The equation used for the calculation of activation energy (E_a) was

$$\ln \ln (1/Y'') = (-E_a/R)\,(1/T) + \text{constant} \qquad (11)$$

where

$$Y'' = (W_t - W\infty) / (W_o - W\infty) \qquad (12)$$

that is, Y'' is the fraction of the number of initial molecules not yet decomposed; W_t is the weight at any time t; W∞ is the weight at infinite time (=zero); and W_o is the initial weight. A plot of ln ln (1/Y'') versus 1/T [eq.(11)] gives an excellent approximation to a straight line over a range of 0.999 > Y'' > 0.001. The slope is related to the activation energy. Representative plots are shown in Figure 3.9(b). The calculated values for the activation energy of

Table 3.4 : Activation Energies of Decomposition of Various Homopolymers and Tercopolymers (using Ozawa Method)

Polymer Samples	Activation Energy, (E_a) (kJ mol^{-1}) (1 - α)[a]			
TP1 {AM-AA-AN (80:10:10)}	61.4 (0.20)	63.6 (0.30)	63.1 (0.35)	60.8 (0.40)
TP2 {AM-AA-AN (60:20:20)}	66.1 (0.20)	62.4 (0.25)	59.7 (0.30)	55.5 (0.45)
TP3 {AM-AA-AN (40:30:30)}	60.3 (0.30)	57.9 (0.35)	55.3 (0.40)	55.3 (0.45)
TP4 {AM-AA-AN (20:40:40)}	168.8 (0.40)	160.4 (0.45)	152.5 (0.50)	156.9 (0.55)
PAM	70.4 (0.25)	70.4 (0.30)	71.3 (0.35)	68.6 (0.40)
PAA	69.9 (0.55)	67.5 (0.60)	70.2 (0.65)	67.7 (0.70)
PAN	112.1 (0.20)	119.4 (0.30)	112.0 (0.35)	112.0 (0.40)

[a] Values of (1-α) are given in parentheses.

decomposition are listed in Table 3.5. The tercopolymers show two-stage decomposition even where AM is 80% in the feed ratio, although the homopolymer PAM shows three-stage decomposition. The first stage of PAM decomposition is not seen in tercopolymer decompositions. In general, tercopolymers require more activation energy for the decomposition than do the homopolymers.

van Krevelen et al.[50] suggested the following equation

$$\ln | \ln (1-C) | = E_a/R\,(T_m+1) \ln T \qquad (n=1) \qquad (13)$$

where, C is $(W_o-W_t)/W_o$ and T_m is the temperature at maximum conversion rate dW/dt. From the corresponding linear plot [Figure 3.10(a)] E_a can be calculated (Table 3.6).

However TG curves for two different heating rates are needed in a method proposed by Reich[51]. The corresponding equation is

$$E_a = 2.303R \log [(B_2/B_1).(T_1/T_2)^2]/(1/T_1-1/T_2) \qquad (14)$$

where B_1 and B_2 are different heating rates, T_1 and T_2 are corresponding temperatures found for each heating rate from TG curves at various percentages of decomposition. The values obtained for activation energy associated with each stage of decomposition are given in Table 3.6.

Furthermore, the energy of activation and order of reaction may be evaluated from a single experimental curve using the Anderson and Freeman (A-F) procedure[52]. The corresponding expression is

$$\Delta \log (dW/dt) = x\,\Delta \log W_r - (E_a/2.303R)\,\Delta(1/T) \qquad (15)$$

where, dW is the change in weight loss corresponding to change in time dt, x is the order of reaction; E_a is the energy of activation; and Wr is the difference in the total weight loss of the process with the weight loss at the particular time

Table 3.5 : Activation Energy of Decomposition for Various Homopolymers and Tercopolymers in Different Ratios by Thermogravimetric Analysis

Polymer Samples	Decomposition Temperature Range (°C)	Weight Loss (%)	Activation Energy[a] ($kJ\ mol^{-1}$)
AM : AA : AN	190-425	24	18.0
(80 : 10 : 10) TP1	433-478	44	65.1
AM : AA : AN	214-399	20	19.9
(60 :20 : 20) TP2	439-489	40	48.9
AM : AA : AN	205-410	16	20.3
(40 : 30 : 30) TP3	436-490	36	58.8
AM : AA : AN	198-326	14	32.7
(20 : 40 : 40) TP4	450-501	42	75.0
PAM	70-204	10	20.3
	305-420	24	23.5
	435-495	58	89.2
PAA	260-359	42	66.0
	435-660	70	13.0
PAN	305-473	16	20.3
	520-844	36	11.8

[a] Calculated using Broido method at a heating rate of 10°C min^{-1} in N_2 atmosphere.

Table 3.6 : Comparison of Activation Energies (kJ mol-1) Obtained by Various Methods

Polymer	Broido		Van Krevelen		Reich		PPS eqn.		Ozawa E_a[b]	A-F method E_a[b]
	E_{a1}	E_{a2}	E_{a1}	E_{a2}	E_{a1}	E_{a2}	E_{a1}	E_{a2}		
PAM	20.3	23.5	21.0	23.9	21.4	40.53	--	--	--	--
	--	89.2[a]	--	87.3[a]	--	87.8	--	--	70.1	79.5
TP1	18.0	65.1	19.5	64.3	27.2	55.6	48.9	79.6	61.5	78.5
TP2	19.9	48.9	20.6	49.9	18.8	42.9	43.1	64.3	60.9	75.4
TP3	20.3	58.8	20.6	58.3	30.1	58.7	50.7	83.6	59.4	64.2
TP4	32.7	75.0	33.4	71.6	28.9	67.5	48.2	75.1	--	57.8
PAA	66.0	13.0	66.4	13.0	60.8	--	50.7	65.9	70.5	48.3
PAN	20.30	11.8	22.4	11.5	--	--	50.7	96.3	--	--

See Table 3.1 and text for symbols.

when dW/dt is considered. A linear plot of Δlog (dW/dt) vs Δ(1/T) gives activation energy E_a [Figure 3.10(c and d)]. The values are given in Table 3.6.

A recently suggested[54] method (PPS eqn) for the determination of activation energy of polymer decomposition uses a single heating rate thermogram. The corresponding equation is

$$dW/dt = -W(S/B)e^{-E/RT} \qquad (16)$$

where, $T = T_o + B_t$, T_o is initial temperature, B is heating rate, W is the initial mass of polymer sample, *S* is frequency factor and E_a is activation energy. The activation energy E_a is derived by minimising the deviation of theoretical points from experimental points [Figure 3.10(b)]. The values obtained for degradation are listed in Table 3.6.

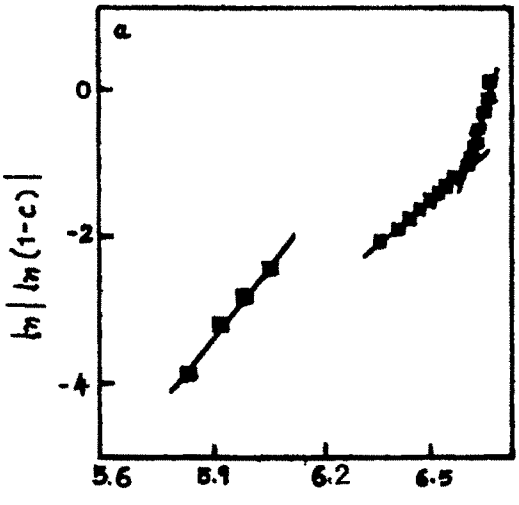

Figure 3.10 (a) : van Krevelen plot for homopolymer PAM at heating rate of 10K min^{-1} in N_2 atmosphere.

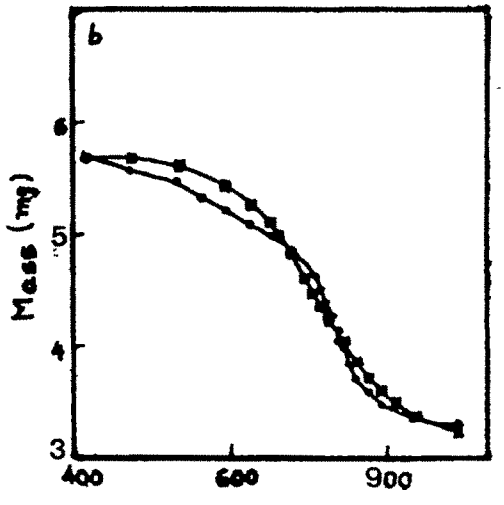

Figure 3.10 (b) : PPS plot for tercopolymer (TP1) at heating rate of 10 K min^{-1} in N_2 atmosphere.
(●) Experimental curve
(■) Theoretical curve.

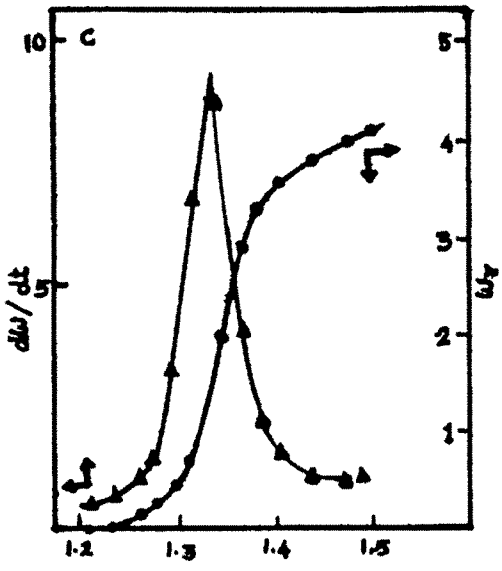

1/T x 10^3 ($^0K^{-1}$)

Figure 3.10 (c) (A-F) : Graph of (▲) the first derivation of the TGA curve (dW/dt) and (●) the weight of reactant (Wr) as a function of reciprocal absolute temperature for the degradation of PAM in N_2 atmosphere.

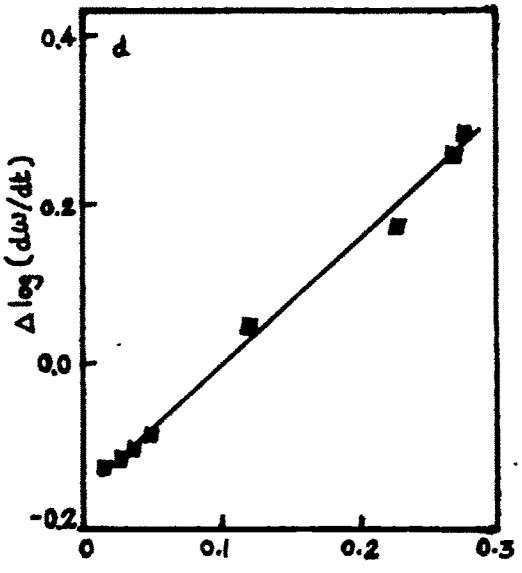

Δ log Wr

Figure 3.10 (d) : Anderson-Freeman plot for kinetics of the thermal degradation of tercopolymer (TP2) in N2 atmosphere at 10 K min^{-1} and taking $\Delta(V_T) = 1.0x10^{-5}$ (K^{-1}).

Table 3.6 shows the kinetic parameters obtained from TG thermogram by using various methods of Broido's, van Krevelen, A-F and PPS eqn using single thermogram at 10K min^{-1} heating rate. It also has results obtained by Reich method by using two heating rates of 10 and 20 K min^{-1} and also results of Ozawa method. As for the activation energy, the values obtained by the methods of Broido and van Krevelen agree very well with each other. The multiple heating rate methods of Ozawa or Reich, yielded reliable values of kinetic parameters, which are in reasonable agreement with the values obtained by former two methods. The PPS eqn yielded higher values of E_a than those obtained by other methods. The possibility of error in A-F method is higher due to the calculation procedure where two stage graphical plots are required to get

activation energy. The PPS eqn is advantageous because of single heating rate, incorporation of various steps of degradation and also that no experimental point is left out. Both Ozawa and A-F methods give only one overall activation energy whereas other methods give activation energies corresponding to different steps of decomposition. Therefore we suggest that depending upon the requirement, the method of calculation could be chosen. A large amount of result in literature is available where Broido method is used. We feel that of all the equations discussed in here and their corresponding results seem to suggest that Broido method is a more useful method among all.

(e) DSC analysis :

DSC scans of various tercopolymers are shown in Figure 3.11. All the samples showed a well pronounced endothermic transition in the temperature range of 135-175°C. The endothermic transition in tercopolymers can be attributed to the anhydride formation reaction as reported by various authors for PAA and its copolymers[43,55]. Polyacrylic acid (PAA) leads to anhydride formation in the temperature range of 170-200°C by a reaction involving adjacent carboxylic acid groups leading to the elimination of water[32]. The T_g of PAA increases with increasing anhydride concentration. Tacticity also plays an important role in deciding the thermal stability and the T_g of PAA. Values of glass transition temperature (T_g) reported for PAA in the literature are 106, 116 and 130°C and for polyacrylamide (PAM) are 84.8 and 165°C respectively, whereas for polyacrylonitrile (PAN) the reported values for T_g is in the range of 85-115°C[56, 57]. The T_g of all these polymers measured by DSC showed variation in T_g of only ± 3°C, which indicates that all these tercopolymers have almost similar structure of polymer backbone and branching of tercopolymer chain is not so pronounced or does not have significant effect on the T_g values.

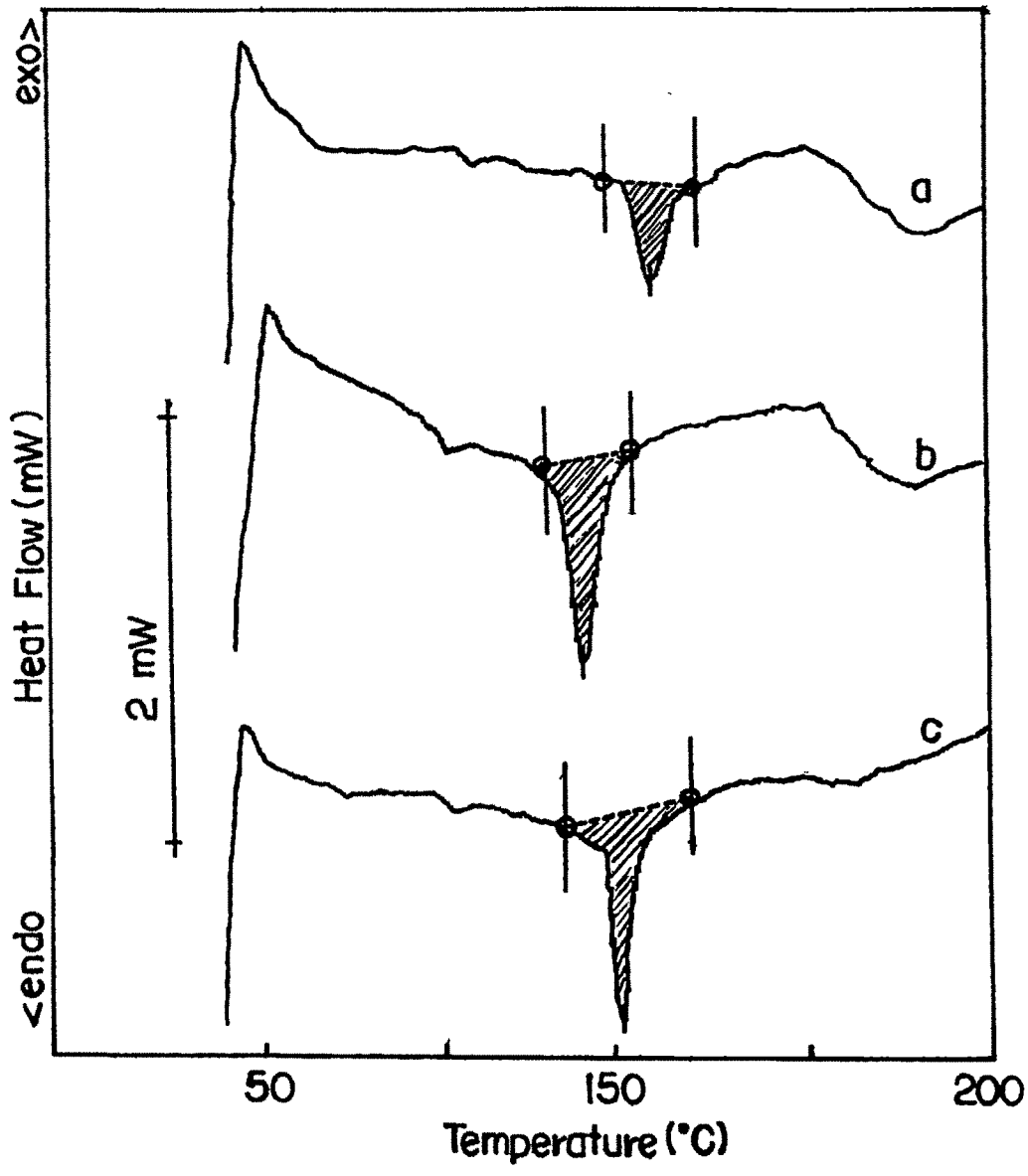

Figure 3.11 : DSC thermogram for tercopolymer (a) TP1, (b) TP2 and (c) TP4 at heating rate of 10 K min^{-1} in N_2 atmosphere.

The values of glass transition temperature (T_g), initial temperature (T_i) /onset temperature (T_o) and peak temperature (T_p) of the endotherm for various

tercopolymers are presented in Table 3.7. The initial temperature is the temperature at which the curve deviates from the base line. It is a measure of initiation of the reaction. The onset temperature is obtained at the intercepts of the tangents to the base line at the lower temperature side of the endothermic peak. Peak temperature is the temperature at which the bulk of the polymer has undergone a dehydration reaction and the difference between the peak temperature and the onset temperature (T_p-T_0) is a measure of the overall rate of reaction. The smaller the difference, the greater the rate of reaction. Another important observation made for DSC scans is enthalpy change associated with endothermic peak, which varies with change in composition of tercopolymers. Tercopolymer containing 56.8 mol% AM shows higher rate of reaction and also enthalpy change was higher in this case than that of the other two tercopolymers (Table 3.7).

(f) Viscosity measurements :

The viscosity behavior of PAM, PAN, and tercopolymers TP1, TP2, TP3 and TP4 was studied at different temperatures of 30, 35 and 40°C. The viscosity studies of PAM and polymer TP1 and TP2 were done in aqueous medium, whereas PAN and polymer TP3 and TP4 were done in DMF. The viscosity of all the tercopolymers was also measured in mixtures of the solvents, that is, various ratios of DMF : H_2O (v/v). The intrinsic viscosity was calculated using the following equations (Huggins and Kraemer) :

$$\eta_{sp}/C = [\eta] + K' [\eta]^2 C \qquad (17)$$

$$\ln \eta_r/C = [\eta] - K'' [\eta]^2 C \qquad (18)$$

where K' and K" are constants for a given polymer / solvent / temperature system. For many linear flexible polymer systems, K' often indicates the

Table 3.7 : Thermal analysis data of the tercopolymers TP1, TP2 and TP4

Terco-polymers	Tercopolymer composition (mol%)			T_g (°C)	Endotherm Range (°C)		Onset Temperature (°C)	Peak Temperature (°C)	T_p-T_o	ΔH (J/g)
	AM	AN	AA		T_i	T_f	T_o	T_p		
TP1	86.1	0.9	13.0	107	145	175	153	159.3	6.3	44.5
TP2	56.8	25.4	17.9	105	135	160	140	144.1	4.1	60.7
TP4	22.4	41.7	35.8	102	135	170	146	150.5	4.5	38.5

See Table 3.1 and text for symbols.

measure of the solvent power; the poorer the solvent, the higher the value of K'. The K'-K" values were found to be around 0.5, as expected[58,59].

The η_{sp}/C values of PAM in H_2O, PAN, and set TP4 in DMF showed a decrease with dilution. When plotted against concentration, straight lines were obtained and intrinsic viscosity values were, hence, computed (Fig. 3.12). For other systems, η_{sp}/C values showed an increase with dilution, and intrinsic viscosity as well as K'-K" values could not be calculated. Intrinsic viscosities of various systems at different temperatures and some representative values of K'-K" are given in Table 3.8.

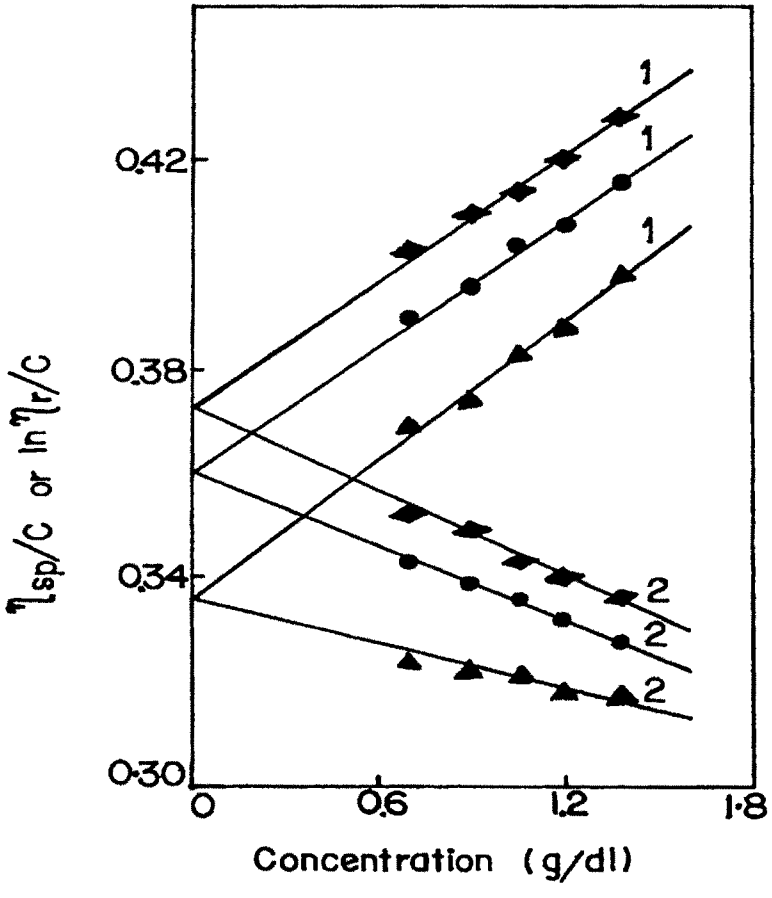

Figure 3.12 : Typical plot of (1) η_{sp}/C and (2) ln η_r/C against concentration (C) for tercopolymer TP4 : (■) 30°C; (●) 35°C ; (▲) 40°C.

Table 3.8 : Intrinsic Viscosities of Various Polymer Systems at Different Temperature in Various Solvents

Polymer Systems / Solvent	A or Intrinsic Viscosity [η] (dL/g)			B			K'-K"
	30°C	35°C	40°C	30°C	35°C	40°C	
PAM/H_2O	--	0.98	2.91	--	--	--	0.51
Set I/H_2O	2.19	2.06	1.96	1.02	0.96	0.91	--
/85 : 15 : : H_2O : DMF	2.17	2.11	2.09	0.88	0.87	0.88	--
/75 : 25 : : H_2O : DMF	2.21	2.14	2.08	0.99	0.96	0.92	--
/40 : 60 : : H_2O : DMF	2.05	2.03	1.97	1.10	1.08	1.05	--
Set II/H_2O	1.33	1.52	1.58	1.04	1.51	1.56	--
/85 : 15 : : H_2O : DMF	1.61	1.59	1.57	1.31	1.31	1.28	--
/75 : 25 : : H_2O : DMF	1.72	1.64	1.57	1.42	1.31	1.21	--
/40 : 60 : : H_2O : DMF	1.70	1.59	1.54	1.23	1.33	1.11	--
Set III/H_2O	1.11	0.99	0.85	1.32	1.24	0.97	--
/50 : 50 : : H_2O : DMF	1.37	1.45	1.48	0.97	1.05	1.13	--
/40 : 60 : : H_2O : DMF	1.58	1.53	1.51	1.11	1.09	1.07	-
/33 : 67 : : H_2O : DMF	1.57	1.53	1.41	1.07	1.09	0.90	--
/25 : 75 : : H_2O : DMF	1.67	1.55	1.45	1.23	1.06	0.97	--
Set IV/H_2O	0.37	0.36	0.34	--	--	--	0.48
/33 : 67 : : H_2O : DMF	0.33	0.36	0.42	0.22	0.23	0.25	--
/25 : 75 : : H_2O : DMF	0.41	0.35	0.34	0.30	0.09	0.09	-
/15 : 85 : : H_2O : DMF	0.45	0.42	0.40	0.17	0.12	0.07	--
PAN / DMF	0.73	0.72	0.71	--	--	--	0.50

The viscosities of various tercopolymers in water, DMF, and a mixture of water : DMF, like other polyelectrolytes, showed a unique dependence on concentration[60], η_{sp}/C values for the above mentioned tercopolymers increased with dilution, contrary to the behavior of nonionic polymers. Representative plots are shown in Figure 3.13(a). As the solution is diluted, the polymer molecules no longer fill all the space and the intervening regions extract some of the mobile ions. Net charges develop in the domains of the polymer molecule, causing them to expand. As this process continues with further dilution, the expansive forces increase. At high dilutions, polymer molecules lose most of their mobile ions and are extended virtually to their maximum length[61]. This leads to high values of η_{sp}/C. Such data can be satisfactorily handled through the use of the empirical relation

$$\eta_{sp}/C = A/(1 + BC^{1/2}) \qquad (19)$$

where A and B are constants. A straight line was obtained on plotting $(\eta_{sp}/C)^{-1}$ against $C^{1/2}$ [Fig. 3.13(b)], where A represents the intrinsic viscosity $(\eta_{sp}/C)_{C\to 0}$[30].

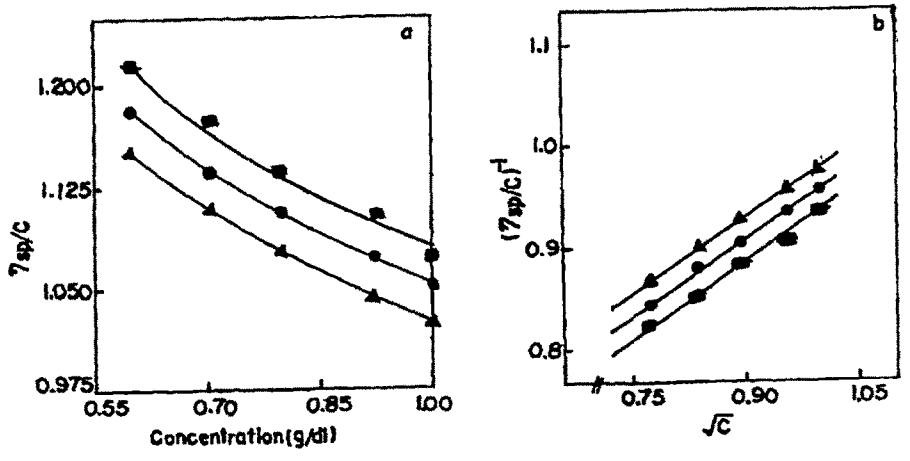

Figure 3.13 : Plot of (a) η_{sp}/C against concentration (C) and (b) $(\eta_{sp}/C)^{-1}$ versus $\sqrt{C}$ for tercopolymer TP1 in water. (■) 30°C; (●) 35°C; (▲) 40°C.

The plot of [η] against the H_2O : DMF ratio (Fig. 3.14) shows a maximum for all the sets of tercopolymers. This indicates that at that maximum of [η] the corresponding H_2O : DMF mixture behaves as a relatively good solvent for the tercopolymers.

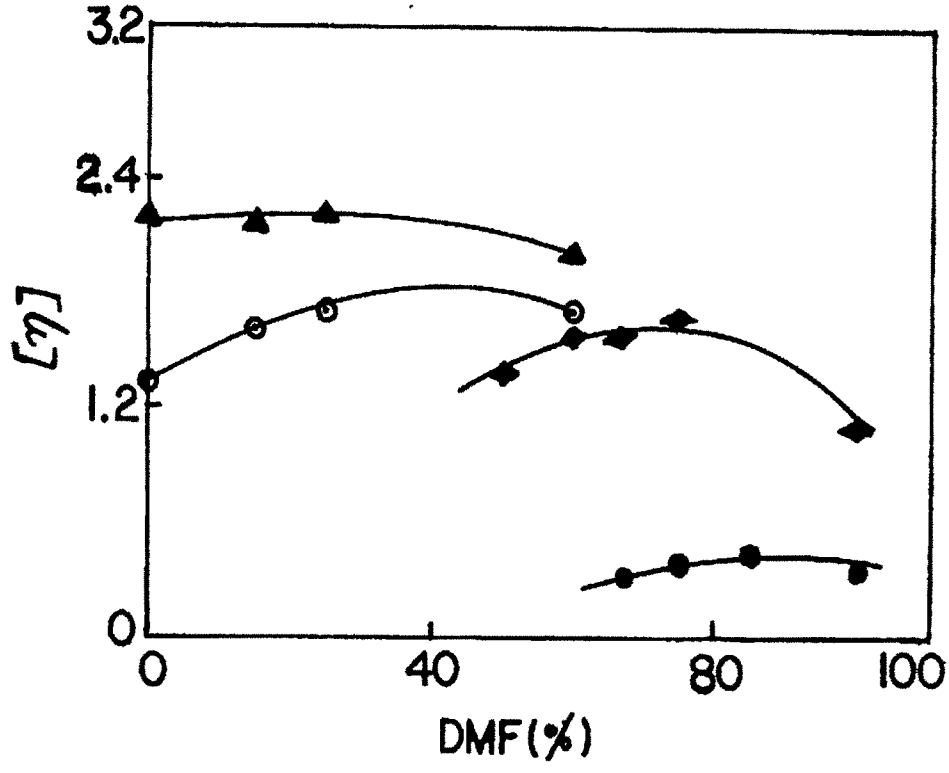

Figure 3.14 : Plot of intrinsic viscosity [η] versus percentage DMF for tercopolymers : (▲) TP1; (■) TP2; (●) TP3.

Relative viscosity data at different concentrations were used for calculations of the voluminosity (V_E) of the polymer solutions, at a given temperature and in different solvent systems[58,59,62] V_E was obtained by plotting χ against concentration C(g dL^{-1}), where (Fig. 3.15)

$$\chi = (\eta_r^{0.5} - 1) / [C (1.35 \eta_r^{0.5} - 0.1) \qquad (20)$$

The straight line then obtained was extrapolated to C = O and the intercept yielded V_E. The values are listed in Table 3.9.

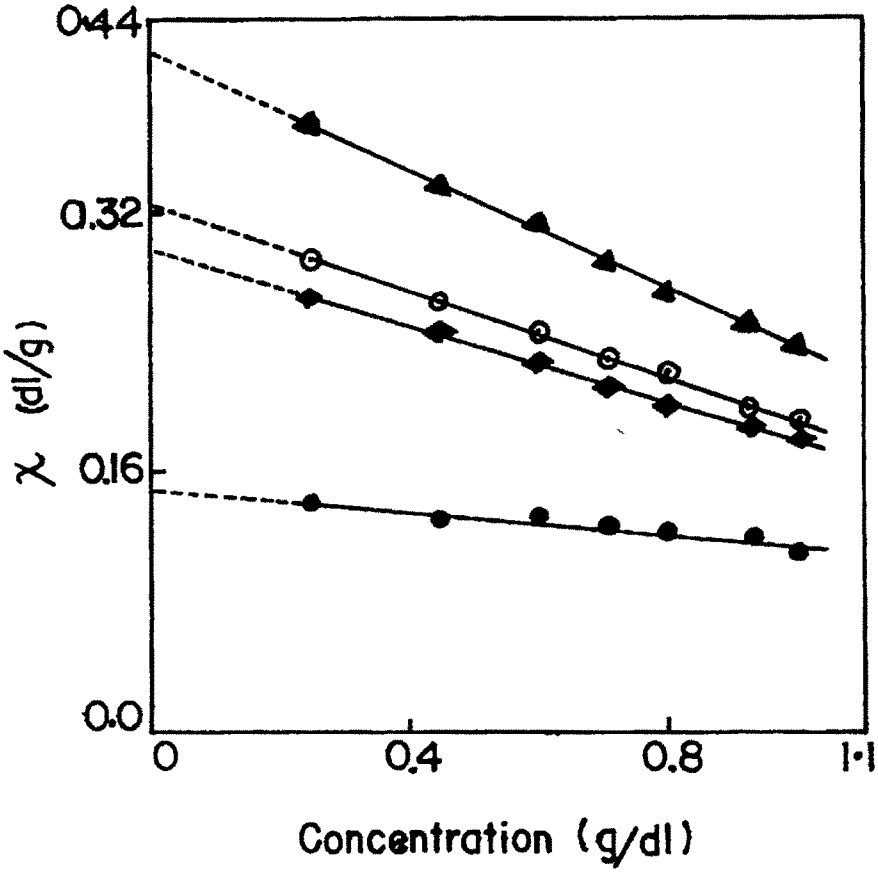

Figure 3.15 : Plot of χ versus concentration (C) for tercopolymers : (▲) TP1 in water; (□) TP2 in DMF : H_2O (60:40); (■) TP3 in DMF : H_2O (50:50); (●) TP4 in DMF.

The shape factor ν was calculated from the equation :

$$[\eta] = \nu V_E \qquad (21)$$

The shape factor gives an idea of the shape of the macromolecules in the solution[63]. The values of the shape factors obtained are given in Table 3.9. All the values for systems behaving normally (PAM in H_2O, PAN and set TP4 in DMF) were found to be around 2.5, indicating a spherical conformation[64] of the

Table 3.9 : Voluminosity (V_E) and Shape Factor (ν) of Various Polymers at Diffeent Temperatures

Polymer Systems / Solvent	30°C		35°C		40°C	
	V_E (dL g^{-1})	ν	V_E (dL g^{-1})	ν	V_E (dL g^{-1})	ν
PAM/H_2O	--	--	1.160	2.5	1.17	2.5
Set I/H_2O	0.421	5.2	0.411	5.0	0.403	4.9
/85 : 15 : : H_2O : DMF	0.438	4.9	0.430	4.9	0.420	4.9
/75 : 25 : : H_2O : DMF	0.428	5.2	0.424	5.0	0.421	5.0
/40 : 60 : : H_2O : DMF	0.394	5.2	0.393	5.2	0.388	5.1
Set II/H_2O	0.312	4.3	0.315	4.8	0.316	5.0
/85 : 15 : : H_2O : DMF	0.309	5.2	0.304	5.2	0.304	5.2
/75 : 25 : : H_2O : DMF	0.314	5.5	0.313	5.2	0.311	5.0
/40 : 60 : : H_2O : DMF	0.326	5.2	0.321	5.0	0.316	4.9
Set III/DMF	0.235	4.7	0.221	4.4	0.206	4.1
/50 : 50 : : H_2O : DMF	0.298	4.6	0.308	4.7	0.303	4.9
/40 : 60 : : H_2O : DMF	0.320	4.9	0.316	4.8	0.314	4.8
/33 : 67 : : H_2O : DMF	0.322	4.9	0.315	4.9	0.313	4.5
/25 : 75 : : H_2O : DMF	0.325	5.2	0.321	4.8	0.314	4.6
Set IV/DMF	0.151	2.5	0.146	2.5	0.136	2.5
/33 : 67 : : H_2O : DMF	0.115	2.9	0.124	2.9	0.139	3.0
/25 : 75 : : H_2O : DMF	0.135	3.0	0.128	2.7	0.126	2.5
/15 : 85 : : H_2O : DMF	0.156	2.9	0.152	2.8	0.147	2.7
PAN / DMF	0.282	2.6	0.277	2.5	0.270	2.6

macromolecules in the solution. The ν values as shown in Table 3.9 were found to be independent of temperature (varying between 2.5 and 2.6). The rest of the systems gave a higher value of ν due to both the complicated distribution in the solution of highly elongated chains and also because of their electrostatic interactions when highly charged. The change in the property of the polymer solution with change in temperature depends upon two antagonistic factors : (i) coiling / uncoiling of polymer chains and (ii) change in the degree of rotation about a skeletal bond[65]. The first one changes the length of the chain, and with increase in temperature, generally increases, leading to higher [η] or higher ν. The second one increases the degree of rotation with increase in temperature and thereby should decrease [η] and, hence, ν. From Table 3.9 it can be seen that the shape factor ν, in general, somewhat decreases, that is, it is oblate spheroid[64] for almost all systems with increase in temperature, indicating a tendency toward spherical conformation at higher temperature.

The voluminosity V_E (dL g^{-1}) is a function of temperature and is a measure of the volume of solvated polymer molecules[63]. As the temperature increases, desolvation takes place and, hence, V_E decreases. In our systems also, V_E values decrease with increase in temperature, indicating desolvation as shown in Table 3.9. For the highly water-soluble tercopolymer TP1, the V_E decreases as the DMF concentration in the mixed solvent increases. For polymer TP2, which is partially water-soluble, V_E increases with increasing percent DMF composition. The same was observed for polymer TP3 and TP4 (Fig. 3.16). For polymer TP1, which is water-soluble, the DMF : water mixture acts as a poor solvent because the V_E value decreases with increase in DMF concentrations. For other sets of polymers (TP2, TP3 and TP4) which are partially water-

soluble or insoluble, the DMF : water mixture is a good solvent to a certain extent since V_E is found to increase with increasing DMF content.

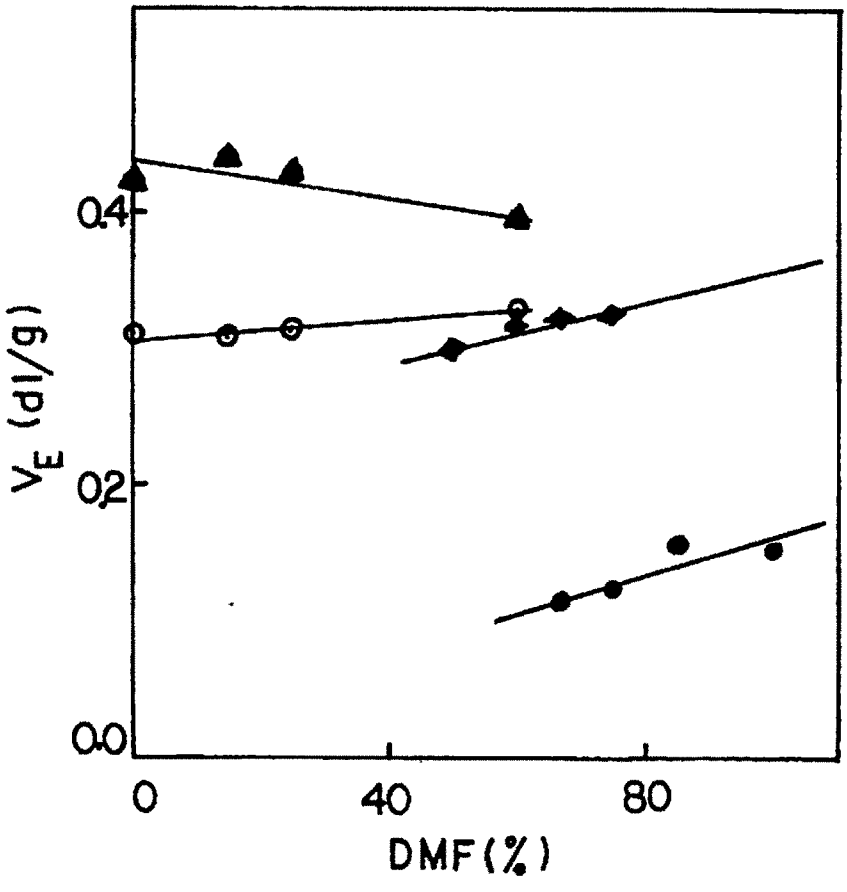

Figure 3.16 : Plot of voluminosity (V_E) versus percentage DMF for tercopolymers.

(g) Biodegradation studies :

When the individual polymer was supplied as a sole carbon and energy source in a synthetic medium, the isolate BA-1 was found to grow on polymer TP1, TP2 and TP3 as shown in Fig.3.17 (a,b,c). The above isolate was found to be gram negative, motile, non-sporeforming, rod shaped bacterium. It also showed oxidase and catalase (enzymic) activity. The isolate did not grow in the absence

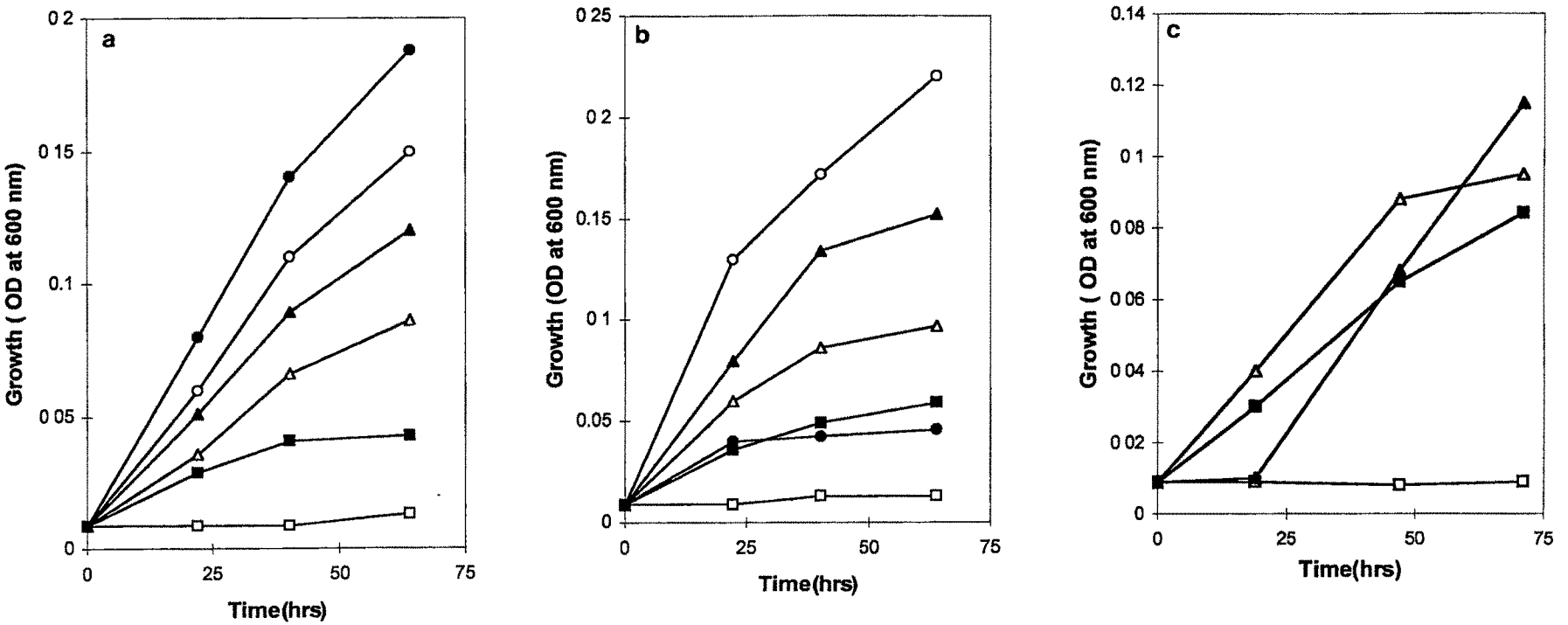

Figure 17 : Time course* of the growth of isolate BA-1 on tercopolymers : a) TP1, b) TP2 and c) TP3. [* Each polymers was supplied as a sole carbon and energy source at a concentration (w/v) of 25% (□), 0.5% (Δ), 1.0% (▲), 2.0% (○) and 4.0% (●). Control (□) had no polymer and was inoculated. In the case of tercopolymer TP3, concentration of 2% and 4% were not tested as medium became turbid at these concentration of the polymer].

of the polymer in the synthetic medium. Thus, for the growth of the isolate BA-1, the presence of the polymer in the medium was found to be essential and thereby indicating the biodegradable nature of these polymers. Using a similar strategy, degradation of copolyesters of citric acid-1,2,6-hexane triol[66] and succinic acid-glycerol-polyethylene glycol-200 copolymer[67] has been reported. The isolate exhibited different degrees of tolerance depending upon the polymer used. In the case of polymer TP1, growth was observed upto 4% (w/v) concentration. In the case of polymer TP2, 2% (w/v) was found to be optimum and higher quantity was found inhibitory. In the case of polymer TP3, the isolate growth was observed, when the polymer concentrations (w/v) were 0.25 % and 0.5%, without a lag period. However, when polymer concentration (w/v) was 1.0 %, the isolate grew with a 20 h lag period. Thus the growth retarding ability of the polymers was found to be in the order polymer TP3 > TP2 > TP1 and this could be due to increased rigidity and decreased hydrophilicity provided by an increased acrylonitrile content. It has been suggested[68] earlier also that the crystalline polymers are more resistant to biodegradation than amorphous ones. Moreover, increase in acrylonitrile content in the polymer also increases the hydrophobicity of the polymer and it has been suggested[19] that the biodegradation of synthetic polymers comprised of biodegradable monomers is usually enhanced by high water solubility of the polymer. This observation was further confirmed by estimating the biomass of growth in terms of whole-cell protein (Table 3.10), where the organism grows best on polymers in the order TP1 > TP2 > TP3.

As aerobic degradation of polymers require the consumption of oxygen, the polymer dependent respiratory activity of the organism observed here indicated the utilisation of the polymer substrates. When the respiratory activity

Table 3.10 : Effect of composition of tercopolymers TP1-TP3 on the growth and respiratory activity of the isolate BA-1

Type of Polymer	Biomass[a] (whole-cell proteim, $\mu g\ mL^{-1}$)	Respiration Rate[b] (μM oxygen consumed min^{-1} mg^{-1} whole-cell protein)
TP1	124.90	99.1
TP2	86.20	61.0
TP3	36.18	38.0

was measured in the presence of polymers TP1, TP2 and TP3, the organisms showed highest respiratory activity in the order polymer TP1 > TP2 > TP3 (Table 3.10), suggesting that the increase of acrylonitrile proportion in the polymer leads to a decrease in respiratory activity. This supported the observation reported on the growth of the isolate on these polymers where increase in acrylonitrile proportion in the polymer retarded the growth and thus reduced the biodegradability.

Gas chromatography was performed to detect the degradation products with a view to elucidate the mechanism of degradation of these polymers. A mechanism proposed[21] for pyrolysis of poly (sodium acrylate) involves a dehydration reaction that occurs by intramolecular cyclization of adjacent structural units which is followed by decarboxylation and chain scission. However, this mechanism which involves formation of cyclic anhydride is suggested to be less likely to occur in microbial metabolism[21], because it was aqueous solution. In our case, two possible mechanisms could be envisaged, one being the hydrolysis of the polymer chains with the release of monomers and their subsequent utilization. When the culture supernatants, after removal of the biomass and unused polymers from the cultures growing on polymer TP1-TP3, were analysed through gas chromatography, the peaks corresponding to acrylic acid, acrylonitrile and acrylamide were found to be absent. As the growth was solely dependent on utilisation of the breakdown products, it is quite likely that these products could have got used up by the growing culture without getting accumulated and this might have led to the failure in detecting them. In fact, a similar observation has been recorded for the aerobic biodegradation of caprolactam where aminocaproic acid, although produced, could not be detected as it was consumed by the growing culture[69].

The second mechanism would probably involve terminal oxidation of the polymers akin to that of β-oxidation of fatty acids as proposed previously[19] for the aerobic degradation of polyacrylates and the degradation by this mechanism cannot be ruled out at the moment.

3.6 Conclusion

On the basis of these results, it can be concluded that the free-radical tercopolymerization reactions of acrylamide, acrylic acid, and acrylonitrile systems follow classic copolymerization theory. The higher reactivity of acrylamide than that of the other two monomers taken together were supported by the reactivity ratios. IR and ^{1}H-NMR spectroscopy provided evidence for the structure of the tercopolymers. ^{13}C-NMR spectroscopy provided evidence for the incorporation of all the three monomeric units i.e. acrylamide, acrylic acid and acrylonitrile in the tercopolymers as well as its compositional and configurational arrangement in the polymer chain. Moreover, enthalpy change associated with polymer TP2 (i.e. 56.8% AM) is higher than that of the other polymers. Almost similar structure of the polymer was found in all the above tercopolymers. The activation energies as well as the shape factors of the tercopolymers that were obtained by TGA and solution viscosity studies. Preliminary studies on biodegradability of the above polymers with a soil bacterial isolate in terms of growth ability and respiratory activity showed that these polymers undergo biodegradation. Increase in the proportion of acrylonitrile in tercopolymers was found to decrease the susceptibility of the polymers to biodegradation with the isolate BA-1.

3.7 References

1) X.Jin, C.Carfagna, L.Nicolais and R.Lanzetta, *Macromolecules,* **28**, 4785 (1995).
2) P.Shukla and A.K.Srivastava, *Polymer,* **35**, 4665 (1994).
3) P.Shukla and A.K.Srivastava, *Macromol. Rep., A,* **31**, 315 (1994).
4) A.A.Mahmoud, A.F.Shaaban, A.A.Khalil, and N.N.Massiha, *Polym. International,* **27**, 333 (1992).
5) G.Kysela and E.Staudner, *J. Polym. Mater.*, **9**, 297 (1992).
6) S.H.Ronnel and D.H.Kohn, *J. Appl. Polym. Sci.*, **19**, 2359 (1975).
7) J.V.Prasad, U.S.Satpathy, M.Jassal, A.Pantar, and S.Satish, *Intern. J. Polymeric Mater.*, **18**, 105 (1992).
8) D.S.G.Hu and M.T.S.Lin, *Polymer*, **35**, 4416 (1994).
9) A-C.Albertsson, *J.M.S.-Pure Appl.Chem.,* **A 30**, 757 (1993).
10) G.S.Kumar, in *Biodegradable Polymers : Prospects and Progress*, Marcel Dikker, Inc., New York, 1987, p.3.
11) K.Sakai, N.Hamada, and Y.Watanabe, *Agric. Biol. Chem.*, **50**, 989 (1986).
12) C.Sakazawa, M.Shimao, Y. Taniguchi, and N.,Kato, *Appl. Environ. Microbiol.*, **41**, 261 (1981).
13) F.Kawai, T.Kimura, M.Fukaya, Y.Tani, K.Ogata, T.Uena, and H.Fukami, *Appl. Environ. Microbiol.*, **35**, 679 (1978).
14) B.Schink, and M.Stieb, *Appl. Environ. Microbiol.*, **47**, 850 (1983).
15) J.E.Potts, in *Kirk-Othmer Encyclopedia of Chem. Technol.*, Suppl.Vol., M.Grayson, (ed.), Wiley Interscience, New York, 1984, p. 626.
16) B.Barim, and R.D.Deanin, *Polym. Plast. Technol. Eng.*, **2**, 1 (1973).
17) J.M.Courtney, R.G.Hood, and J.M.Ewart, *J. Appl. Polym. Sci.*, **23**, 1449 (1979).

18) F.Kawai, K.Igarashi, and F.Kasuya, *J. Environ. Polym. Degn.*, **2**, 59 (1994).

19) E.Rittman , J.A.Suftin, and B.Henry, *Biodegradation*, **2**, 181(1992).

20) F.Leonard, R.K.Kulkarni, G.Brandes, J.Nelson, and J.Cameron, *J. Appl. Polym. Sci.*, **10**, 259 (1960).

21) T.Hayashi, M.Mukouyama, K.Sakano, and Y.Tani, *Appl. Environ. Microbiol.*, **59**, 1555 (1993).

22) N.Kunichika, T.Ooi, and S.Kinoshita, *J. Ferm. Bioeng.*, **84**, 213 (1997).

23) F.A.Bovey, and L.W.Jelinski, *Chain Structure and Conformation of Macromolecules*, Academic Press, New York, 1982.

24) J.C.Randall, *Polymer Sequence Determination*, Academic Press, New York, 1977.

25) K.D.Chapatwala, E.M.Hall, and G.R.V.Babu, *World Journal of Microbiology and Biotechnology*, **9**, 483 (1993).

26) G.D.Barron, *Methods in Microbiology.* Vol.4, J.R.Norris, and D.W.Ribbons, (eds), Academic Press, London, 1971, p. 405.

27) D.Herbert, P.J.Phipps, and R.F.Strange, *Methods in Microbiology*,Vol.5B J.R.Norris, and D.W.Ribbons, (eds), Academic Press, London, 1971, p. 250.

28) A.S.Teot, in *Encyclopedia of Chemical Technology*, Vol.20, M.Grayson, Ed., Wiley, New York, 1980, p.217.

29) J.D.Morris and R.J.Penzenstadler, in *Encyclopedia of Chemical Technology*, Vol.10, M.Grayson, Ed., Wiley, New York, 1980, p.321.

30) W.M.Thomas, in *Encyclopedia of Polymer Science and Technology*, Vol.1, H.F.Mark, N.G.Gaylord and N.M.Bikales, Eds., Wiley, New York, 1964, p.181.

31) R.Joseph, S.Devi and A.K.Rakshit, *J. Appl. Polym. Sci.*, **50**, 173 (1993).

32) P.Bajaj, M.Goyal, and R.B.Charan, *J. Appl. Polym. Sci.*, **51**, 423 (1994).

33) F.Candau, Z.Zekhnini, F.Heatley and E.Franta, *Colloid Polym. Sci.*, **264**, 676 (1986).

34) P.Bajaj, K.Sen, and H.S.Bahrami, , *J. Appl. Polym. Sci.*, **59**, 1539 (1996).

35) T.Kelen and F.Tudos, J. *Makromol. Sci. Chem.*, **9**, 1 (1975).

36) M.Fineman and S.Ross, *J. Polym. Sci.*, **5**, 259 (1980).

37) N.A.Granem, N.A.Massiha, , N.E.Ikladious and A.F.Shaaban, *J. Appl. Polym. Sci.*, **26**, 97 (1981).

38) C.L.McCormick and G.S.Chen, *J. Polym. Sci.*, **22**, 3633, 3649 (1984).

39) C.L.McCormick and K.P.Blackmon, *Polymer*, **27**, 1971 (1986).

40) S.Igarshi, *J. Polym. Sci. Polym. Lett. Ed.*, **1**, 359 (1963).

41) J.Schaefer, *J. Macromol.*, **4**, 105 (1971).

42) R.M.Silverstein, R.G.Bessler, and T.C.,Morrill, *Spectroscopic Identification of organic Compounds*, 4th ed., Wiley, New York, 1981.

43) D.H.Grand and N.Grassie, *Polymer*, **1**, 125 (1960).

44) L.M.Minsk, C.K.Chik, G.N.Meyer and W.O.Kenyon, *J. Polym. Sci. Polym. Ed.*, **12**, 133 (1974).

45) M.Tutas, M.Saglam, M.Yuksel and C.Guler, *Thermochim. Acta*, **111**, 121 (1987).

46) T.Ozawa, *J. Therm. Anal.*, **2**, 301 (1970).

47) T.Ozawa, *Bull. Chem. Soc. Jpn.*, **38**, 1881 (1965).

48) H.Nishizaki, K.Yoshida and J.H.Wang, *J. Appl. Polym. Sci.*, **25**, 2869 (1980).

49) A.Broido, *J. Polym. Sci.*, **7**, 1761 (1969).

50) D.W.van Krevelen, C.van Heerden and F.J.Huntjens, *Fuel*, **30**, 253 (1951).

51) L.Reich, *J. Polym. Sci. Polym. Lett. Ed.*, **2**, 621 (1964).

52) D.A.Anderson and E.S.Freeman, *J. Polym. Sci.* **54**, 253 (1961).

53) P.K.Chatterjee, *J. Polym. Sci. Part A*, **3**, 4253 (1965).

54) A.Pratap, V.Potbhare and V.Shrinet, submitted to Polymer (1999).

55) J.J.Maurer, D.J.Kustace, and C.T.Ratcliffe, *Macromolecules*, **20**,196 (1987).

56) A.Rangaraj, V.Vangani, and A.K.Rakshit, *J. Appl. Polym. Sci.*, **66**, 45 (1997).

57) J.Brandrup, and E.H.Immergut, *Polymer Handbook*, 3rd ed, Wiley, New York, 1989.

58) V.Vangani and A.K.Rakshit, *J. Appl. Polym. Sci.*, **45**, 1165 (1992).

59) R.Joseph, S.Devi and A.K.Rakshit, *Polym. Int.*, **26**, 89 (1991).

60) T.Ogawa and M.Sakai, *J. Appl. Polym. Sci.*, **23**, 2817 (1979).

61) P.J.Flory, *Principles of Polymer Chemistry*, 1st ed., Cornell University Press, New York, 1953, p.635.

62) S.Ajitkumar, D.Prasadkumar, S.Kansara and N.K.Patel, *Eur. Polym. J.*, **31**, 149 (1995).

63) H.H.Kohler and J.Strand, *J. Phys. Chem.*, **94**, 7628 (1990).

64) G.V.Vinogradov and A.Ya.Malkin, *Rheology of Polymers*, Mir, Moscow, 1980.

65) M.Bhagat, S.Joshi, S.S.Kansara and N.K.Patel, *J. Polym. Mater.*, **14**, 159 (1997).

66) D.Pramanik, T.T.Ray, and M.A.Bakr, *J. Polym. Mater.*, **13**, 173 (1996).

67) M.A.Bakr, M.M.Ali, and P.K.Sarkar, *J. Polym. Mater.*, **14**, 251 (1997).

68) P.J.Hocking, *J.M.S. Rev. Macromol. Chem. Phy.*, **C 32**, 35 (1992).

69) G.Shama, and D. A.Wase, *J. International Biodeterioration Bulletin*, **17**, 1 (1981).